Supplement of Biogeosciences, 22, 4405–4422, 2025
https://doi.org/10.5194/bg-22-4405-2025-supplement

Biogeosciences Open Access EGU

Supplement of

Particulate inorganic carbon pools by coccolithophores in low-oxygen–low-pH waters off the Southeast Pacific margin

Francisco Javier Díaz-Rosas et al.

Correspondence to: Francisco Javier Díaz-Rosas (fjdiaz4@uc.cl)

Supplementary Section S1. Tables

Table S1: Coccolith length measurements used to estimate specific PIC_{Cocco} quotas.

Species or genus	Length (µm)	Volume ($µm^3$)	Mass (pg)	Coccoliths measured
Gephyrocapsa parvula	2.0 ± 0.1	0.4	1.0	6
Gephyrocapsa huxleyi	3.6 ± 0.3	0.9	2.5	20
Gephyrocapsa oceanica	5.2 ± 0.6	6.9	18.7	20
Helicosphaera spp.	9.0 ± 1.1	36.9	99.7	20
Oolithotus spp.	4.5 ± 0.4	6.2	16.8	20
C. leptoporus large-type	8.1 ± 0.9	41.9	113.0	20
C. leptoporus small-type	3.9 ± 0.4	4.7	12.6	11
Syracosphaera spp.	3.7 ± 0.2	0.8	2.0	2
Acanthoica spp.	4.0 ± 0.3	1.9	5.2	5
Discosphaera tubifera	1.6 ± 0.1	0.3	0.8	2
Umbellosphaera spp.	5.7 ± 0.6	2.7	7.4	7
Umbilicosphaera spp.	4.7 ± 0.6	5.1	13.9	7

Table S2: Pairwise comparisons of surface PIC values among the OMZ and other regions based on robust ANOVA with 20 % trimmed means (Yuen's method). The table includes test statistics, 95 % confidence intervals, p-values, and significance levels ($p < 0.05$ marked with asterisks). OMZ – Oxygen Minimum Zone; ATL – Atlantic Ocean; SOC – Southern Ocean; IND – Indian Ocean; ART – Western Arctic; PAT – Patagonian Shelf.

Comparison	Test statistic	CI_lower	CI_upper	*p*-value	Significance
OMZ vs ATL	-0.329	-0.646	0.137	0.0496	*
OMZ vs SOC	-3.552	-4.669	-2.575	<0.001	***
OMZ vs IND	-1.637	-2.075	-1.151	<0.001	***
OMZ vs ART	0.104	-0.262	0.565	0.497	ns
OMZ vs PAT	-3.543	-4.257	-2.833	<0.001	***
ATL vs SOC	-3.224	-4.33	-2.353	<0.001	***
ATL vs IND	-1.308	-1.586	-1.047	<0.001	***
ATL vs ART	0.433	0.254	0.591	<0.001	***
ATL vs PAT	-3.214	-3.842	-2.668	<0.001	***
SOC vs IND	1.915	1.026	3.024	<0.001	***
SOC vs ART	3.656	2.778	4.762	<0.001	***
SOC vs PAT	0.009	-1.091	1.195	0.972	ns
IND vs ART	1.741	1.449	2.057	<0.001	***
IND vs PAT	-1.906	-2.596	-1.27	<0.001	***
ART vs PAT	-3.647	-4.265	-3.093	<0.001	***

Table S3: Pairwise comparisons of surface POC values among the OMZ and other regions based on robust ANOVA with 20 % trimmed means (Yuen's method). The table includes test statistics, 95 % confidence intervals, *p*-values, and significance levels ($p < 0.05$ marked with asterisks). OMZ – Oxygen Minimum Zone; ATL – Atlantic Ocean; SOC – Southern Ocean; IND – Indian Ocean; ART – Western Arctic; PAT – Patagonian Shelf.

Comparison	Test_statistic	CI_lower	CI_upper	*p*-value	Significance
OMZ vs ATL	-0.018	-0.021	-0.015	<0.001	***
OMZ vs SOC	-0.028	-0.038	-0.02	<0.001	***
OMZ vs IND	-0.034	-0.039	-0.03	<0.001	***
OMZ vs ART	0.001	-0.001	0.004	0.113	ns
OMZ vs PAT	-0.021	-0.026	-0.017	<0.001	***
ATL vs SOC	-0.01	-0.02	-0.002	<0.001	***
ATL vs IND	-0.016	-0.02	-0.012	<0.001	***
ATL vs ART	0.019	0.017	0.022	<0.001	***
ATL vs PAT	-0.004	-0.008	0.001	0.022	*
SOC vs IND	-0.006	-0.014	0.005	0.116	ns
SOC vs ART	0.03	0.022	0.039	<0.001	***
SOC vs PAT	0.007	-0.002	0.017	0.0384	*
IND vs ART	0.035	0.032	0.04	<0.001	***
IND vs PAT	0.012	0.007	0.018	<0.001	***
ART vs PAT	-0.023	-0.028	-0.019	<0.001	***

Table S4: Pairwise comparisons of surface PIC:POC ratios among the OMZ and other regions based on robust ANOVA with 20 % trimmed means (Yuen's method). The table includes test statistics, 95 % confidence intervals, *p*-values, and significance levels ($p < 0.05$ marked with asterisks). OMZ – Oxygen Minimum Zone; ATL – Atlantic Ocean; SOC – Southern Ocean; IND – Indian Ocean; ART – Western Arctic; PAT – Patagonian Shelf.

Comparison	Test_statistic	CI_lower	CI_upper	*p*-value	Significance
OMZ vs ATL	-0.018	-0.021	-0.015	<0.001	***
OMZ vs SOC	-0.028	-0.038	-0.02	<0.001	***
OMZ vs IND	-0.034	-0.039	-0.03	<0.001	***
OMZ vs ART	0.001	-0.001	0.004	0.113	ns
OMZ vs PAT	-0.021	-0.026	-0.017	<0.001	***
ATL vs SOC	-0.01	-0.02	-0.002	<0.001	***
ATL vs IND	-0.016	-0.02	-0.012	<0.001	***
ATL vs ART	0.019	0.017	0.022	<0.001	***
ATL vs PAT	-0.004	-0.008	0.001	0.022	*
SOC vs IND	-0.006	-0.014	0.005	0.116	ns
SOC vs ART	0.03	0.022	0.039	<0.001	***
SOC vs PAT	0.007	-0.002	0.017	0.0384	*
IND vs ART	0.035	0.032	0.04	<0.001	***
IND vs PAT	0.012	0.007	0.018	<0.001	***
ART vs PAT	-0.023	-0.028	-0.019	<0.001	***

Table S5: Pairwise comparisons of subsurface PIC values among the OMZ and other regions based on robust ANOVA with 20 % trimmed means (Yuen's method). The table includes test statistics, 95 % confidence intervals, *p*-values, and significance levels ($p < 0.05$ marked with asterisks). OMZ – Oxygen Minimum Zone; ATL – Atlantic Ocean; SOC – Southern Ocean; IND – Indian Ocean; ART – Western Arctic.

Comparison	Test_statistic	CI_lower	CI_upper	*p*-value	Significance
OMZ vs ATL	-0.44	-0.631	-0.255	<0.001	***
OMZ vs SOC	-3.368	-7.418	-1.381	<0.001	***
OMZ vs IND	-1.496	-1.933	-1.132	<0.001	***
OMZ vs ART	0.005	-0.281	0.249	0.956	ns
ATL vs SOC	-2.928	-6.996	-0.99	<0.001	***
ATL vs IND	-1.057	-1.47	-0.675	<0.001	***
ATL vs ART	0.445	0.159	0.693	<0.001	***
SOC vs IND	1.872	-0.18	5.946	0.0108	*
SOC vs ART	3.373	1.383	7.415	<0.001	***
IND vs ART	1.501	1.06	1.944	<0.001	***

Table S6: Pairwise comparisons of subsurface POC values among the OMZ and other regions based on robust ANOVA with 20 % trimmed means (Yuen's method). The table includes test statistics, 95 % confidence intervals, *p*-values, and significance levels ($p < 0.05$ marked with asterisks). OMZ – Oxygen Minimum Zone; ATL – Atlantic Ocean; SOC – Southern Ocean; IND – Indian Ocean; ART – Western Arctic.

Comparison	Test_statistic	CI_lower	CI_upper	*p*-value	Significance
OMZ vs ATL	16.277	10.969	22.491	<0.001	***
OMZ vs SOC	5.09	-11.462	15.754	0.284	ns
OMZ vs IND	18.048	10.725	25.529	<0.001	***
OMZ vs ART	16.992	5.121	25.777	<0.001	***
ATL vs SOC	-11.187	-27.788	-1.81	<0.001	***
ATL vs IND	1.771	-4.186	6.645	0.373	ns
ATL vs ART	0.714	-10.164	6.915	0.834	ns
SOC vs IND	12.958	1.907	30.034	<0.001	***
SOC vs ART	11.901	-2.549	29.061	0.0196	*
IND vs ART	-1.056	-12.448	7.602	0.747	ns

Table S7: Pairwise comparisons of subsurface PIC:POC ratios among the OMZ and other regions based on robust ANOVA with 20 % trimmed means (Yuen's method). The table includes test statistics, 95 % confidence intervals, *p*-values, and significance levels ($p < 0.05$ marked with asterisks). OMZ – Oxygen Minimum Zone; ATL – Atlantic Ocean; SOC – Southern Ocean; IND – Indian Ocean; ART – Western Arctic.

Comparison	Test_statistic	CI_lower	CI_upper	*p*-value	Significance
OMZ vs ATL	-0.032	-0.039	-0.026	<0.001	***
OMZ vs SOC	-0.078	-0.163	-0.038	<0.001	***
OMZ vs IND	-0.081	-0.102	-0.062	<0.001	***
OMZ vs ART	-0.006	-0.017	-0.001	0.002	**
ATL vs SOC	-0.046	-0.131	-0.005	0.0012	**
ATL vs IND	-0.049	-0.071	-0.029	<0.001	***
ATL vs ART	0.027	0.015	0.034	<0.001	***
SOC vs IND	-0.003	-0.048	0.083	0.912	ns
SOC vs ART	0.072	0.032	0.16	<0.001	***
IND vs ART	0.075	0.053	0.097	<0.001	***

Table S8: Robust two-sample comparisons of PIC and POC values along with PIC:POC ratios between the two OMZ layers using 10 % trimmed means. Reported values include test statistics, 95 % confidence intervals, *p*-values, and significance levels ($p < 0.05$ marked with asterisks).

Variable	Test statistic	CI_lower	CI_upper	*p*-value	Significance
PIC	3.676	0.334	1.075	0.0016	**
POC	4.519	44.995	132.574	<0.001	***
PIC:POC	-2.298	-0.006	-0.001	0.0174	*

Supplementary Section S2. Figures

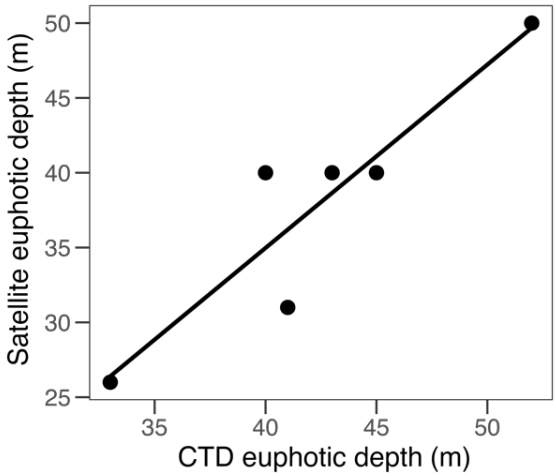

Figure S1: Comparison between euphotic depth derived from satellite observations and from PAR obtained with a sensor attached to the CTD. The solid black line represents the fitted linear regression.

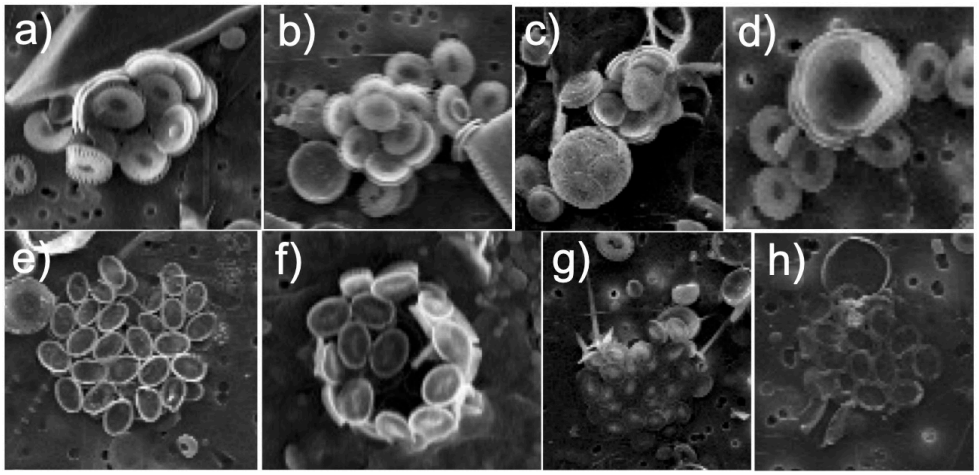

Figure S2: Zoom of scanning electron microscopy images showing layers of coccoliths detached from *G. huxleyi* (a-c), as well as, collapsed coccospheres of different species with distinct brightness (d-h).

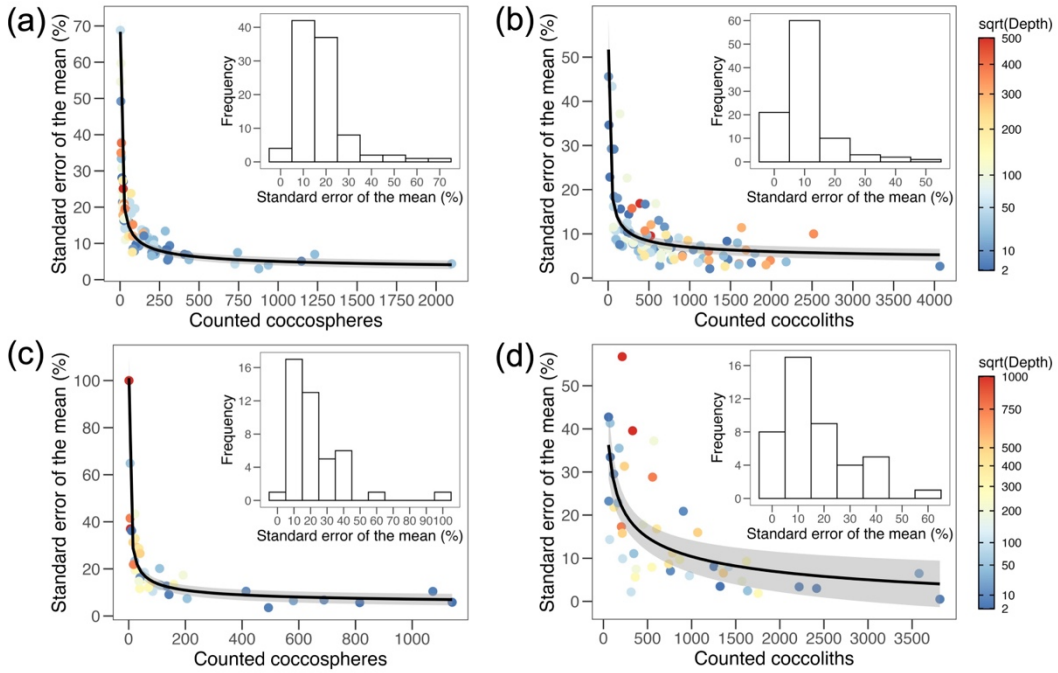

Figure S3: Relationship across depth between the total coccospheres and detached coccoliths counted for each sample, with the standard error of the mean (SE, in %) calculated from images of the same sample. Cross-polarized light microscopy (a-b) and scanning electron microscopy (c-d). Inset histograms show the frequency distribution of SE values. The solid black line represents the fitted hyperbolic curve, with shaded grey areas indicating the 95% confidence intervals. Counts and SEs showed a significant hyperbolic relationship for coccospheres (a) $y = 2.070\ (\pm 0.655) + 93.779\ (\pm 3.301)\ 1/x^{0.5}$; $R^2_{adjusted} = 0.89$; $p\text{-value}_{slope,\ constant} < 0.05$, and detached coccoliths obtained with cross-polarized light microscopy (b) $y = 3.569\ (\pm 0.771) + 107.676\ (\pm 9.141)\ 1/x^{0.5}$; $R^2_{adjusted} = 0.59$; $p\text{-value}_{slope,\ constant} < 0.05$, as well as, coccospheres (c) $y = 4.091\ (\pm 1.318) + 96.968\ (\pm 5.284)\ 1/x^{0.5}$; $R^2_{adjusted} = 0.89$; $p\text{-value}_{slope,\ constant} < 0.05$, and detached coccoliths obtained with scanning electron microscopy (d) $y = -8.785\ (\pm 4.714) + 152.344\ (\pm 27.065)\ 1/x^{0.3}$; $R^2_{adjusted} = 0.42$; $p\text{-value}_{slope} < 0.05$.

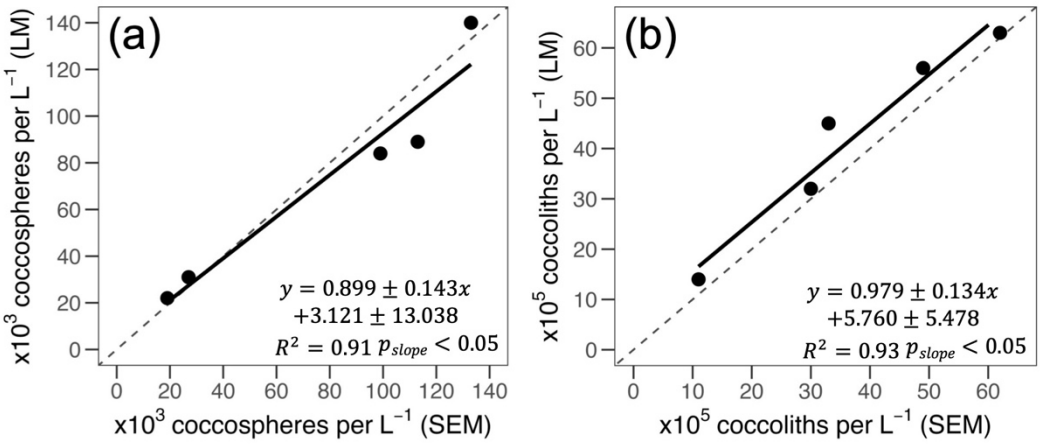

Figure S4: Linear relationships for coccosphere counts (a) and detached coccolith counts (b) obtained through Scanning Electron Microscopy (SEM) and cross-polarized light microscopy (LM). The dotted line represents the 1:1 relationship, while the solid black line and shaded grey areas depict the empirical trend and 95 % confidence intervals.

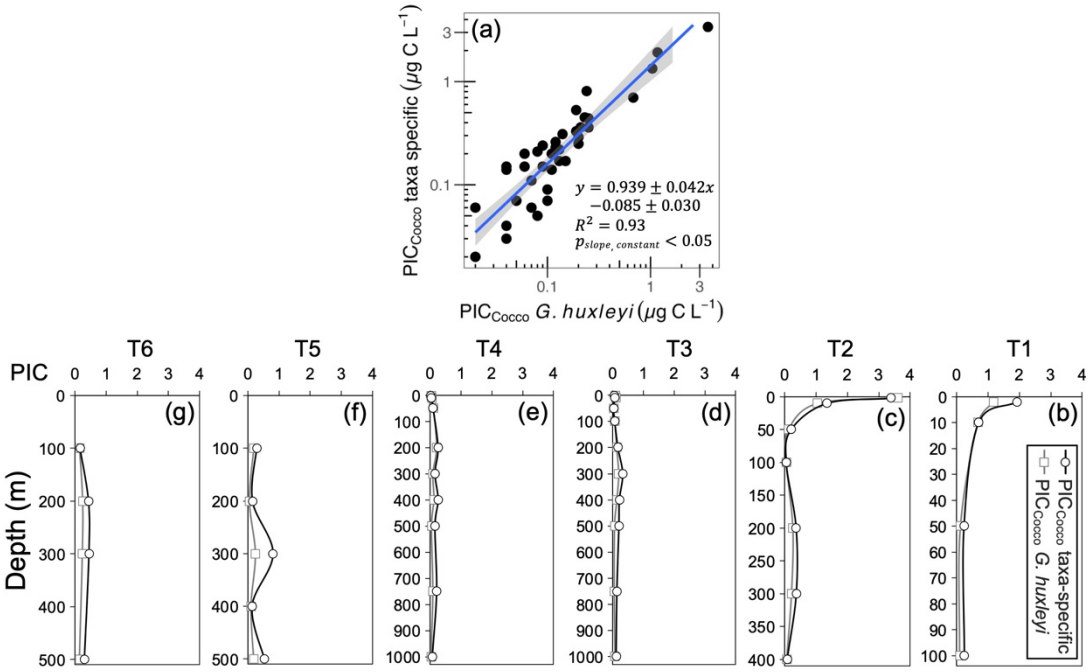

Figure S5: Scatterplot (a) and depth profiles (b-g) comparing PIC_{Cocco} estimates derived from *G. huxleyi* coccolith mass conversion versus taxon-specific shape factors along the 2015 inshore-offshore transect. PIC values are expressed in µg L^{-1}. The solid blue line in scatterplot (a), shown on a log-log scale, represents the fitted linear regression, with shaded grey areas indicating the 95% confidence intervals.

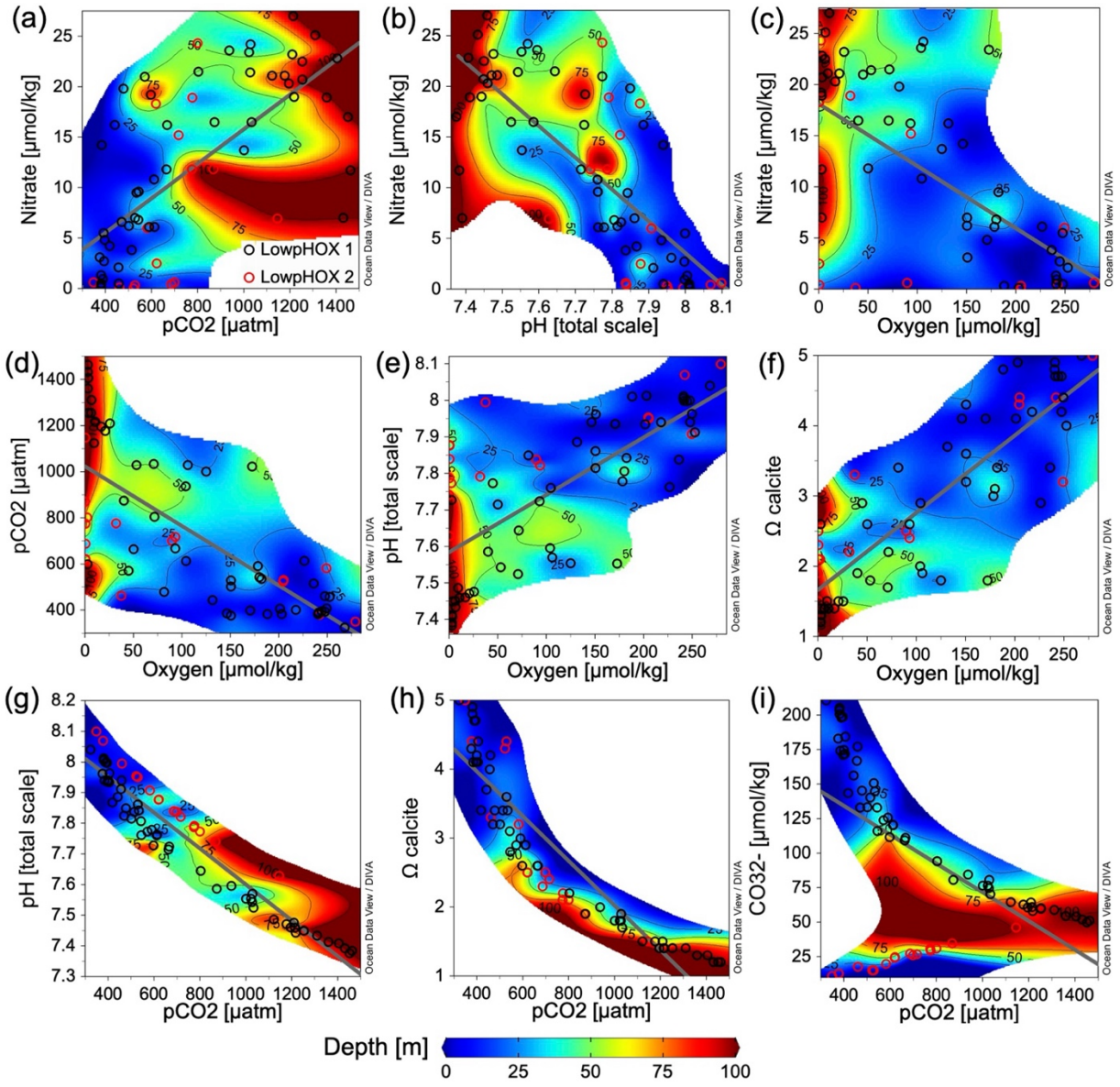

Figure S6: Variation in nitrate vs pCO_2 (a), pH (b), and O_2 (c), along with variation in O_2 vs pCO_2 (d), pH (e), and $\Omega_{calcite}$ (f), plus pCO_2 vs pH (g), $\Omega_{calcite}$ (h), and carbonate ion (i) within 100 m depth during late-spring 2015 (open black dots) and mid-summer 2018 (open red dots). The gray line depicts the least-square model fit curve. pCO_2 vs nitrate $y = 0.0171\ (\pm 0.00036)x - 1.335\ (\pm 0.298)$; $R^2 = 0.68$; $n = 67$. pH vs nitrate $y = -31.366\ (\pm 0.593)x + 254.5\ (\pm 4.59)$; $R^2 = 0.76$; $n = 67$. O_2 vs nitrate $y = -0.061\ (\pm 0.00137)x + 18.12\ (\pm 0.195)$; $R^2 = 0.65$; $n = 62$. O_2 vs pCO_2 $y = -2.582\ (\pm 0.00129)x + 1023\ (\pm 0.194)$; $R^2 = 0.74$; $n = 66$. O_2 vs pH $y = 0.00157\ (\pm 0.00129)x + 7.584\ (\pm 0.194)$; $R^2 = 0.73$; $n = 66$. O_2 vs $\Omega_{calcite}$ $y = 0.011\ (\pm 0.0013)x + 1.66\ (\pm 0.194)$; $R^2 = 0.86$; $n = 66$. pCO_2 vs pH $y = -0.00059\ (\pm 0.00035)x + 8.186\ (\pm 0.282)$; $R^2 = 0.96$; $n = 71$. pCO_2 vs $\Omega_{calcite}$ $y = -0.00324\ (\pm 0.00035)x + 5.26\ (\pm 0.282)$; $R^2 = 0.91$; $n = 71$. pCO_2 vs carbonate ion $y = -0.104\ (\pm 0.00035)x + 176\ (\pm 0.282)$; $R^2 = 0.58$; $n = 71$.

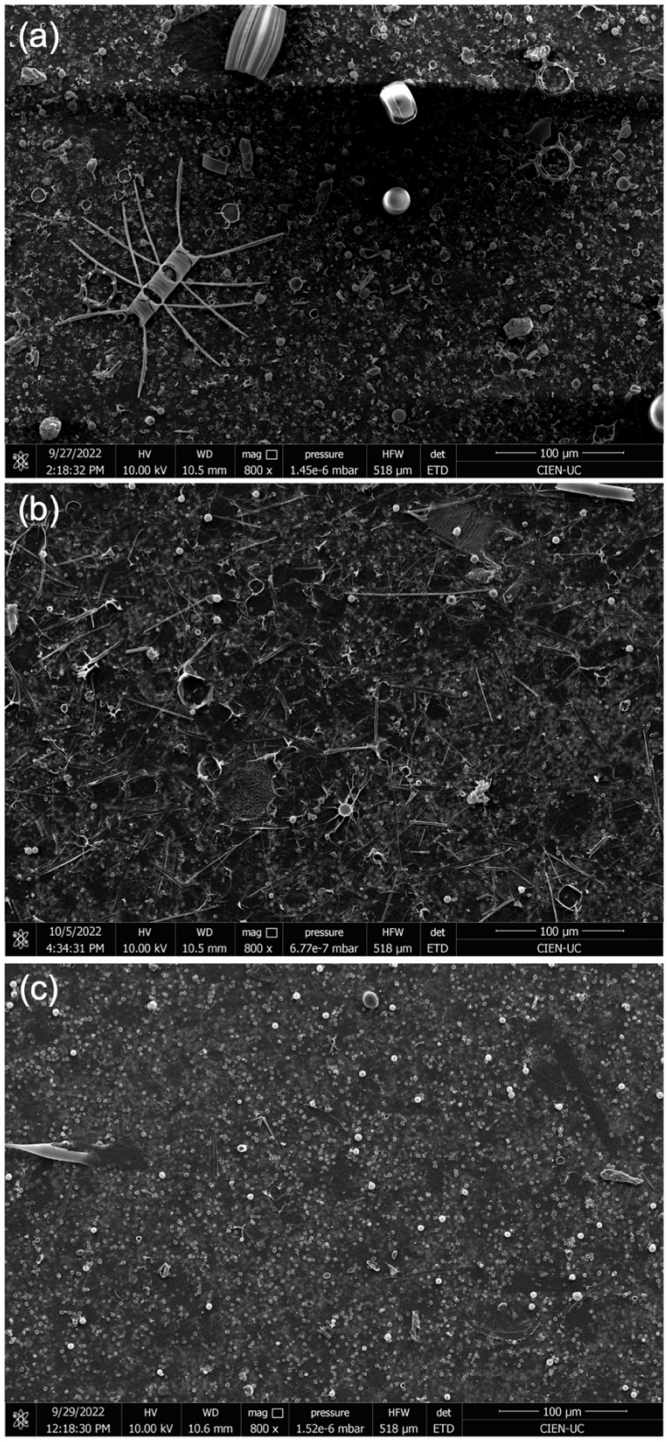

Figure S7: Scanning electron microscopy showing diverse coccolithophore and diatom assemblages in 2015 station T1 at 2 m depth (a) as well the dominance of coccospheres and detached-coccoliths of *G. huxleyi* during post-bloom of diatoms in 2015 station L2 at 5 m depth (b) and under low biomass conditions in 2015 station L3 at 5 m depth (c). Each 800x frame corresponds to 0.2 mm^2.

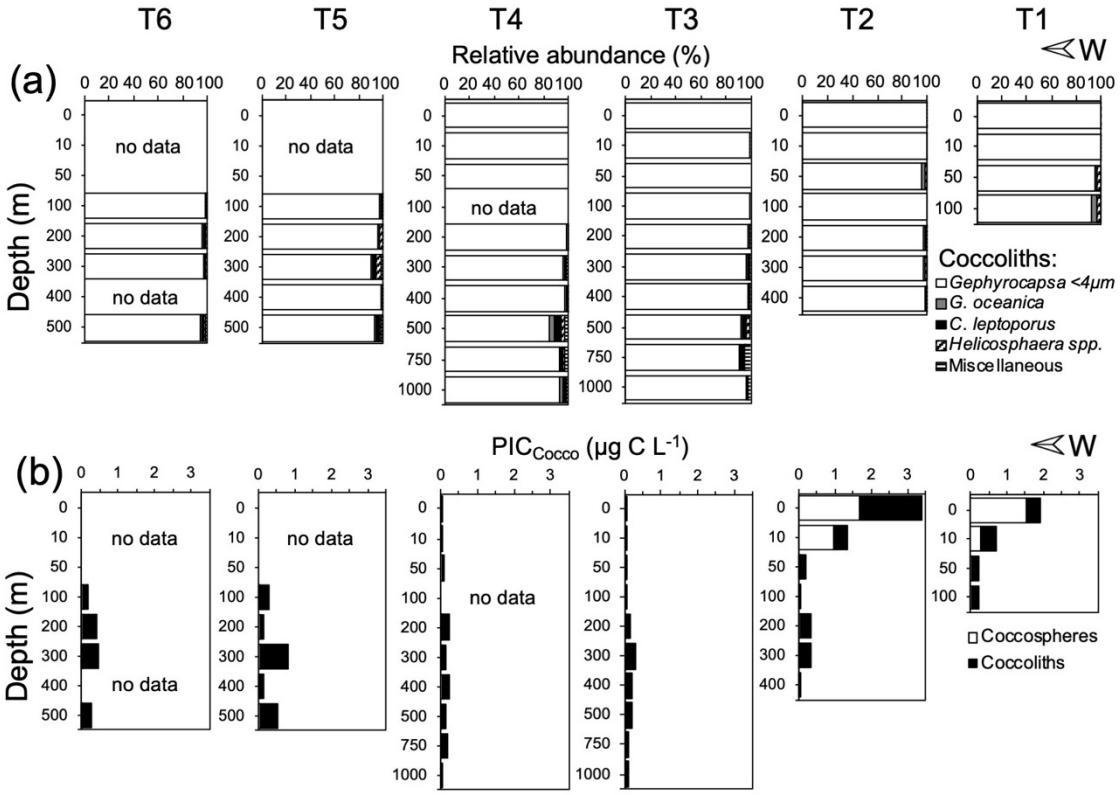

Figure S8: Relative abundances of detached coccoliths (a) and contribution of coccospheres and detached coccoliths to the total PIC_{Cocco} pool (b) in waters off Iquique (20º S) during late-spring 2015. In panels (b) the PIC_{Cocco} pool estimate is derived from abundances obtained through scanning electron microscopy.

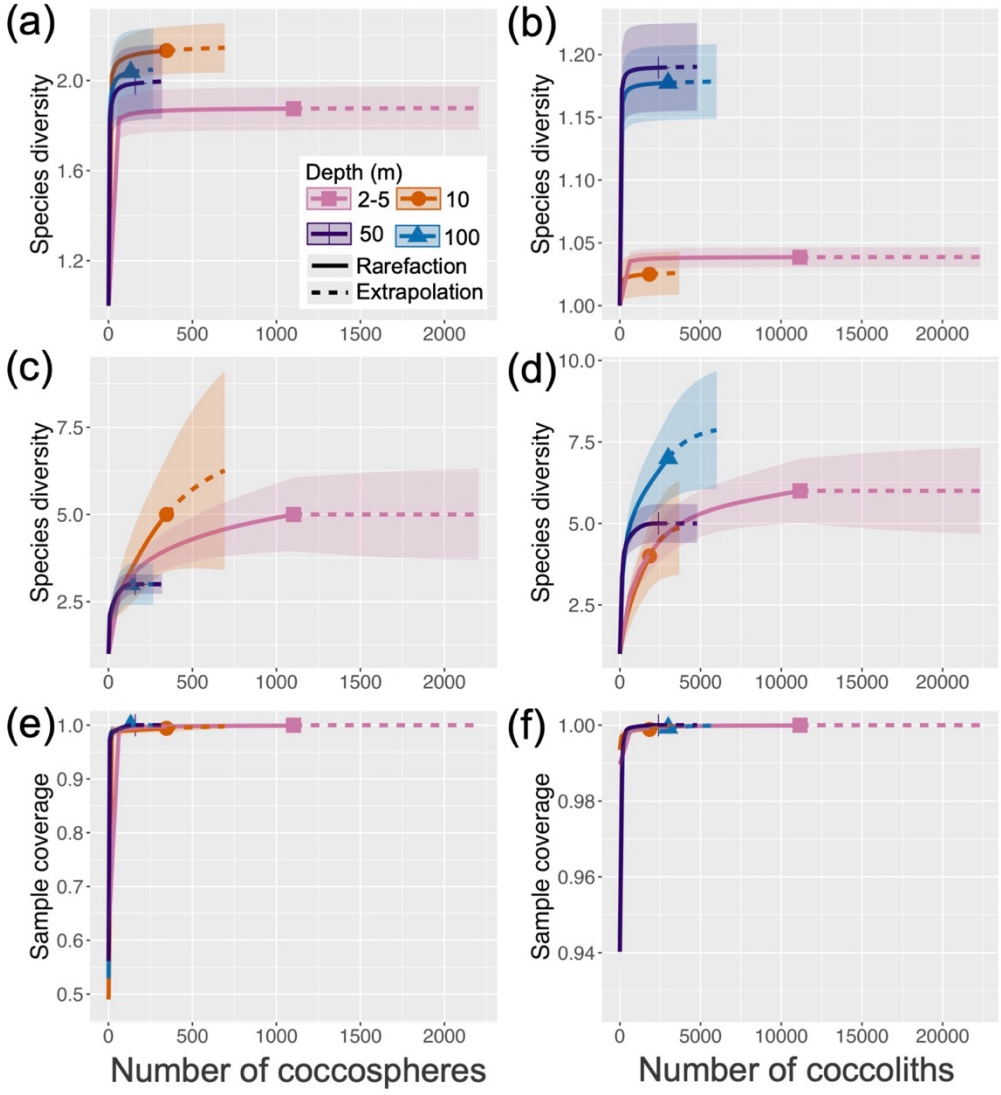

75

Figure S9: Rarefaction-extrapolation analysis for late-spring 2015 and mid-summer 2018, showing species richness (a-b), the exponential of Shannon entropy (c-d), and sample completeness (e-f) for coccospheres and detached coccoliths observed at 2-5, 10, 50, and 100 m. Each curve in plots a-d includes 95 % confidence intervals.

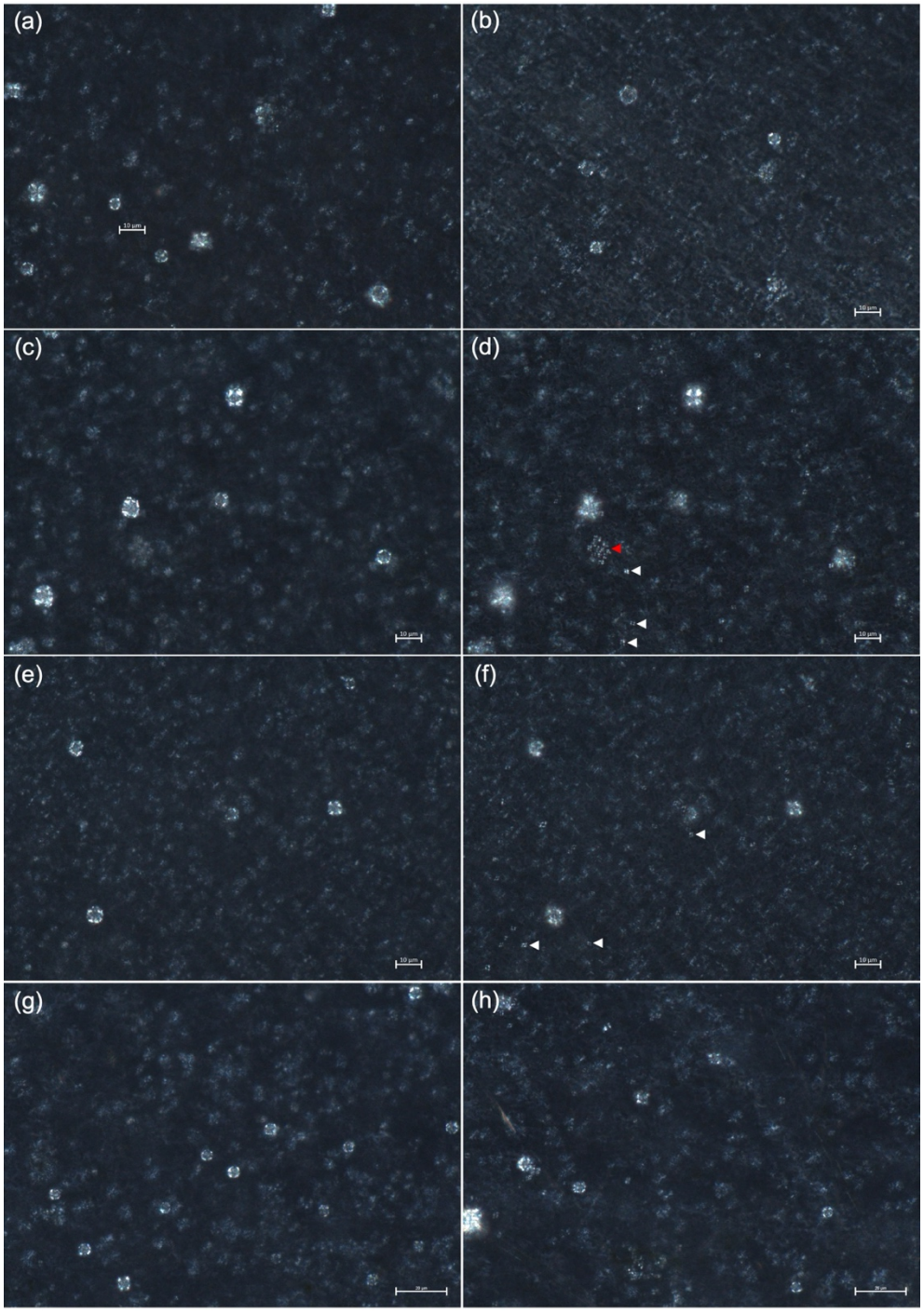

Figure S10: Cross-polarized light microscopy showing coccospheres and detached coccoliths of *G. huxleyi* dominating during mid-summer 2018. Images corresponding to: (a) Station Hyd3 at 25 m depth, (b) Station Hyd4 at 50 m depth, (c and d) Station Hyd6 at 10 m depth different focus, (e and f) Station Lander1 (La1) at 15 m depth with distinct focus, (g) Station T5 at 30 m depth, and (h) Station T5 at 30 m depth. Note the white arrows in (d) and (f) indicate some detached coccoliths, and red arrow in (d) a layer of coccoliths included in detached-coccoliths counts. All images taken at 630x magnification.

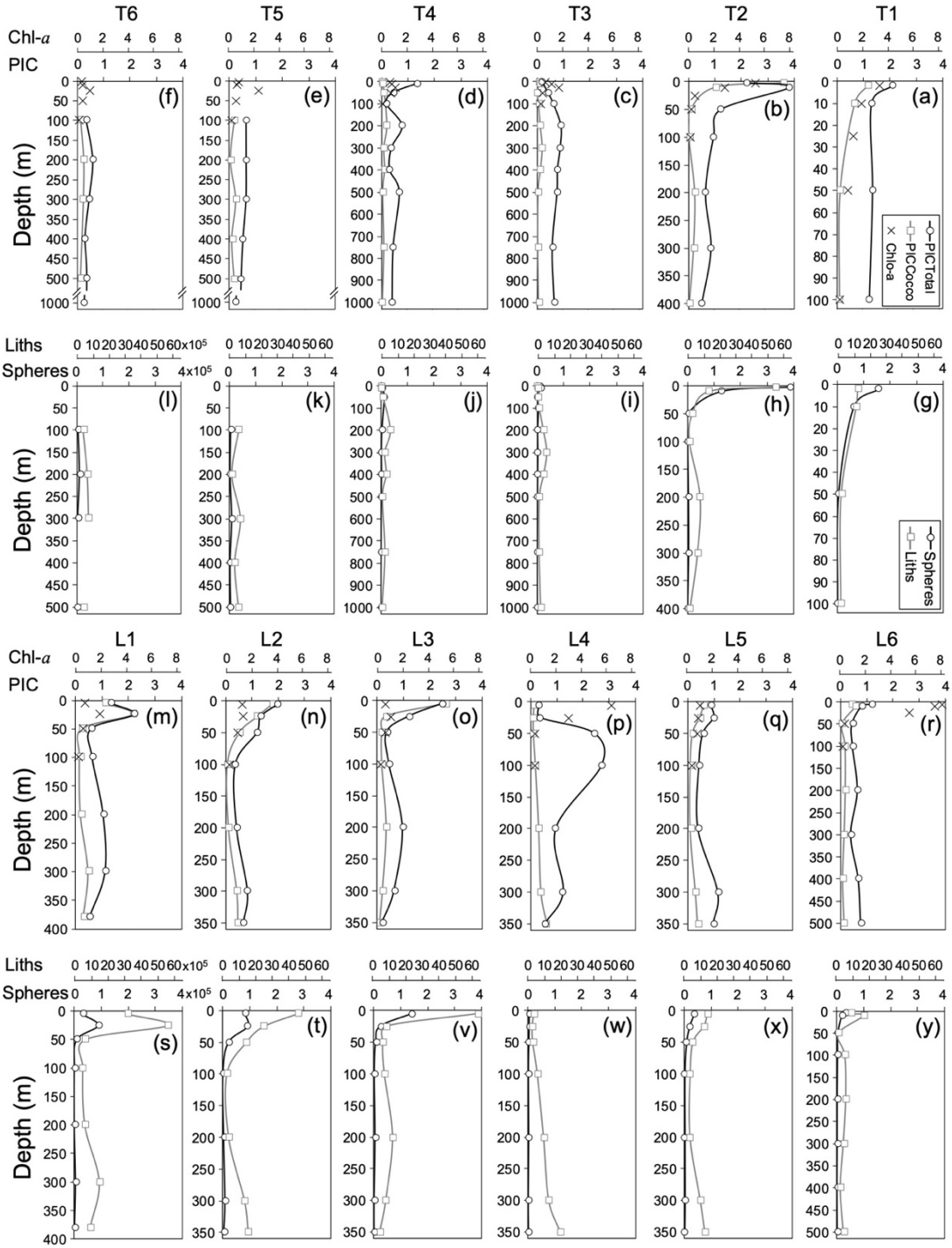

Figure S11: Profiles of PIC_{Total}, PIC_{Cocco}, Chl-*a*, coccospheres, and detached coccolith along the inshore-offshore transect (a-l) and the latitudinal leg (m-y) sampled in late-spring 2015. Note that the axes for each variable span the same range. Both PIC and Chl-*a* values are expressed in µg L^{-1}.

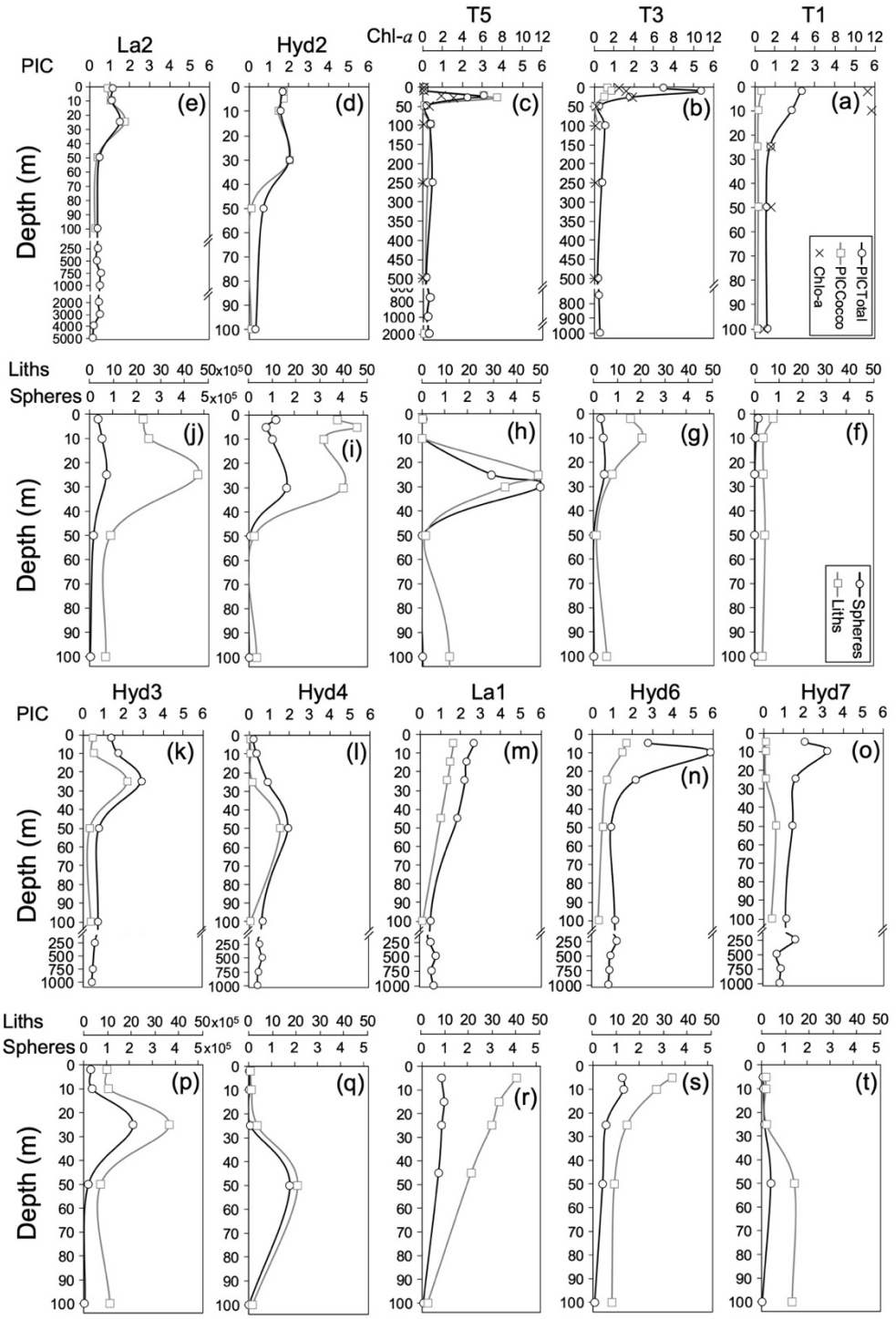

Figure S12: Profiles of PIC_{Total}, PIC_{Cocco}, Chl-*a*, coccospheres, and detached coccoliths along the inshore-offshore transect (a-c, f-h) and the latitudinal leg (d-e, i-t) sampled in mid-summer 2018. Note that the axes for each variable span the same range. Both PIC and Chl-*a* values are expressed in µg L^{-1}.

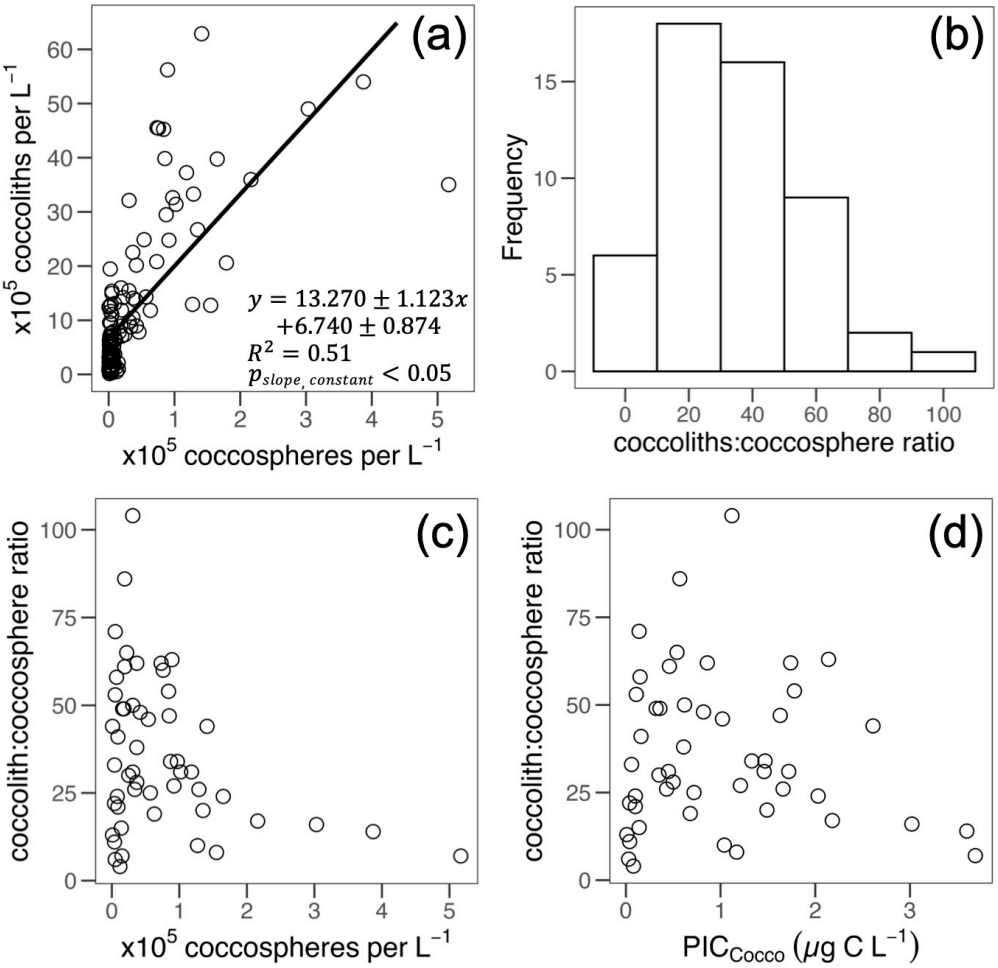

Figure S13: Linear relationship between (a) coccospheres and detached coccoliths, (b) histogram of detached coccolith-to-coccosphere ratio frequencies, and relationships between (c) coccospheres and detached coccolith-to-coccosphere ratios, and (d) PIC_{Cocco} and detached coccolith-to-coccosphere ratios recorded during late-spring 2015 and mid-summer 2018. The solid black line in (a) represents the fitted linear regression.

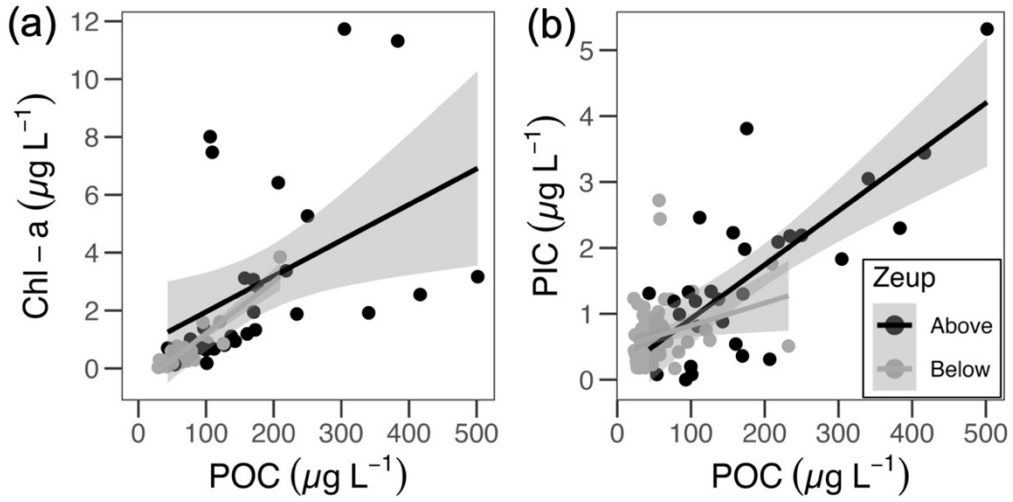

Figure S14: Chl-*a* vs POC and PIC vs POC data variation above and below the euphotic zone. The solid black lines represent the fitted linear regression, with shaded grey areas indicating the 95% confidence intervals. POC vs Chl-*a* above Z_{eu} $y = 0.012\ (\pm 0.005)x + 0.717\ (\pm 1.026\ )$; $R^2_{(adjusted)}$ = 0.17; *p*-value$_{(slope)}$ < 0.05; *n* = 29. POC vs Chl-*a* below Z_{eu} $y = 0.018\ (\pm 0.002)x - 0.602\ (\pm 0.109\ )$; $R^2_{(adjusted)}$ = 0.82; *p*-value$_{(slope,\ constant)}$ < 0.05; *n* = 32. POC vs PIC above Z_{eu} $y = 0.008\ (\pm 0.001)x + 0.106\ (\pm 0.298\ )$; $R^2_{(adjusted)}$ = 0.54; *p*-value$_{(slope)}$ < 0.05; *n* = 29. POC vs PIC below Z_{eu} $y = 0.003\ (\pm 0.001)x + 0.478\ (\pm 0.088)$; $R^2_{(adjusted)}$ = 0.06; *p*-value$_{(slope,\ constant)}$ < 0.05; *n* = 76.

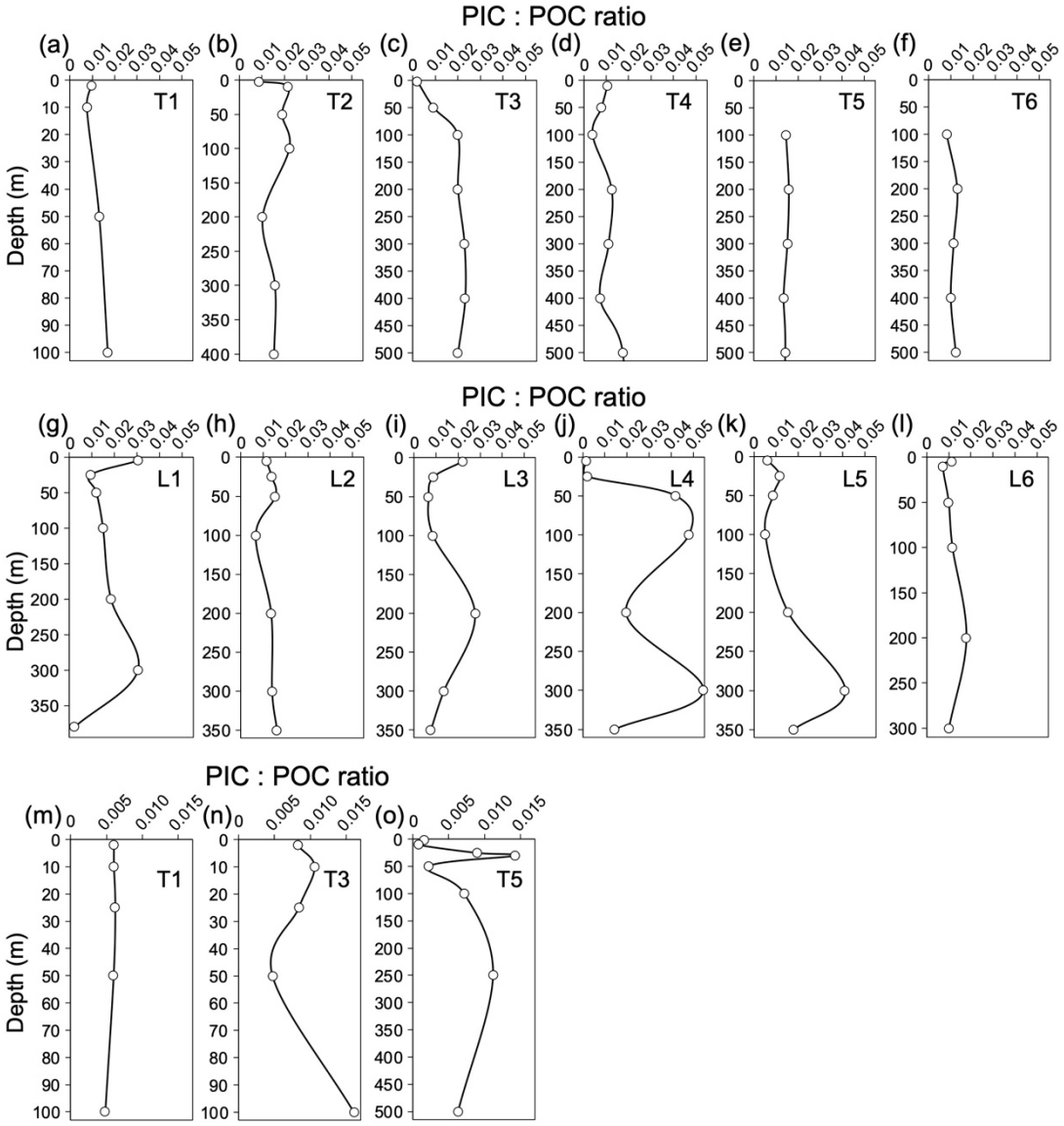

Figure S15: Profiles of PIC:POC ratios across the inshore-offshore transect (a-f) and latitudinal leg (g-l) sampled in late-spring 2015, as well as across the inshore-offshore transect (m-o) sampled in mid-summer 2018.

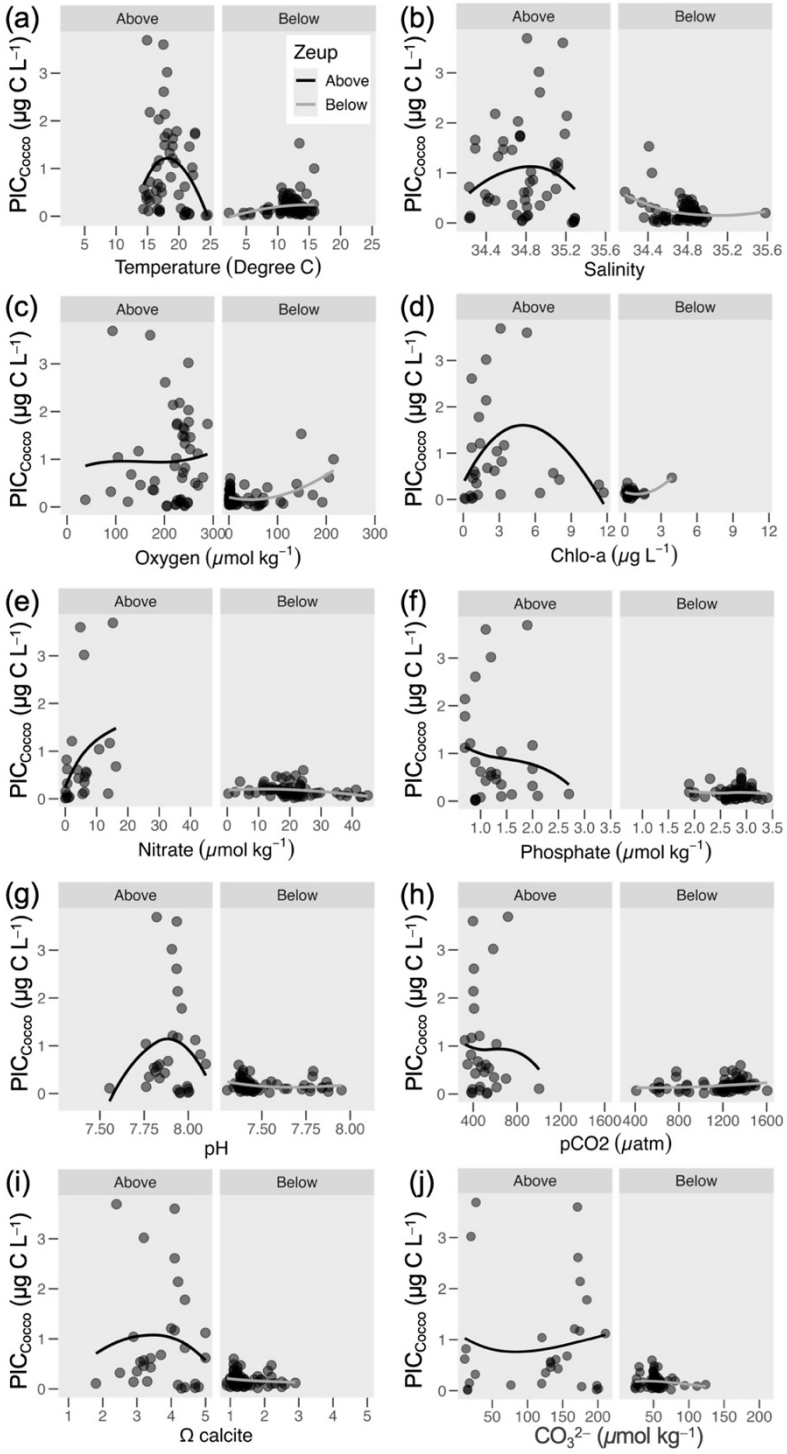

Figure S16: Variation in PIC_{Cocco} above and below the euphotic zone across environmental conditions during late-spring 2015 and mid-summer 2018. Temperature (a), Salinity (b), O_2 (c), Chl-*a* (d), nitrate (e), phosphate (f), pH (g), pCO_2 (h), $\Omega_{calcite}$ (i), and carbonate ion (j) are shown.

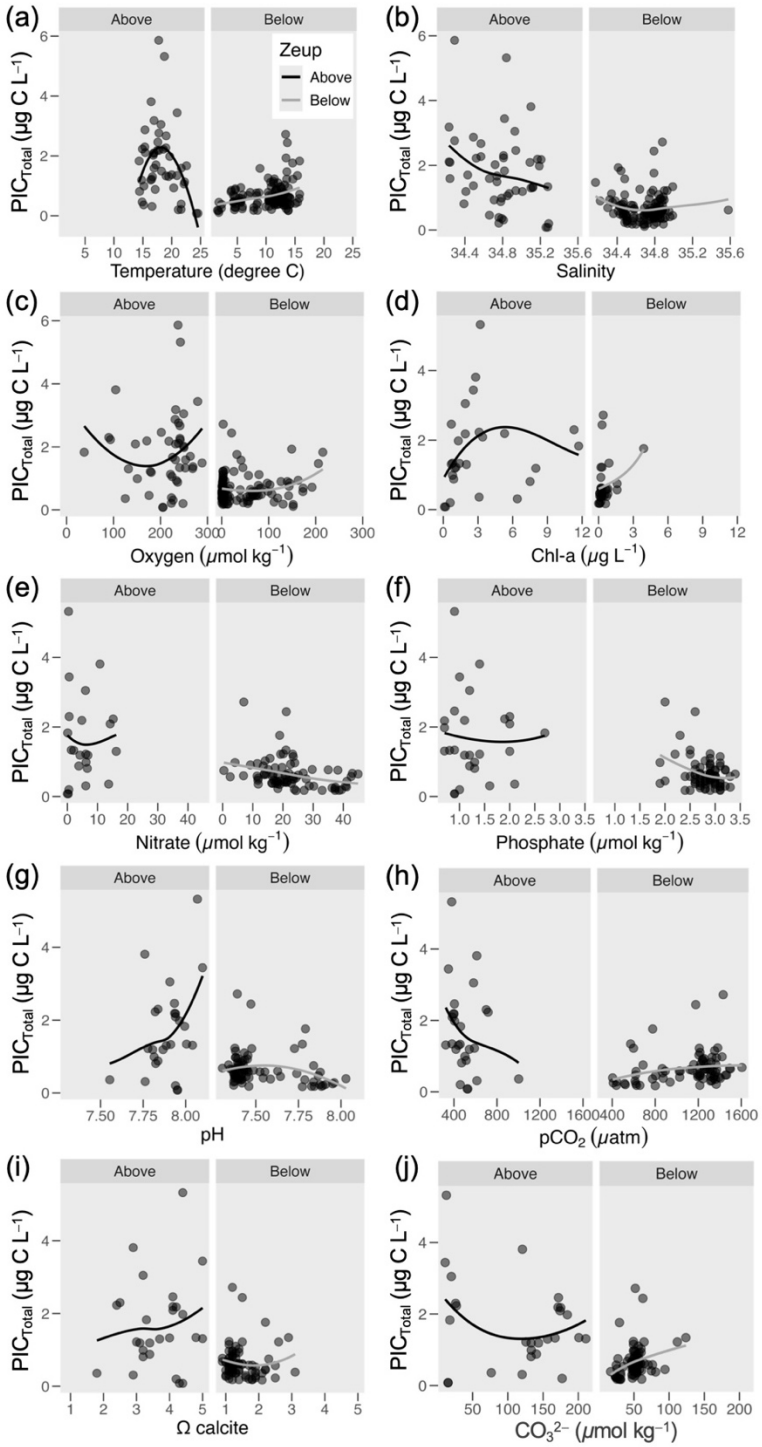

Figure S17: Variation in PIC_{Total} above and below the euphotic zone across environmental conditions during late-spring 2015 and mid-summer 2018. Temperature (a), Salinity (b), O_2 (c), Chl-*a* (d), nitrate (e), phosphate (f), pH (g), pCO_2 (h), $\Omega_{calcite}$ (i), and carbonate ion (j) are shown.